Edinburgh Research Explorer

Analysis of the magnetoencephalograrn background activity in Alzheimer's disease patients with auto-mutual information

Analysis of the magnetoencephalogram background activity in Alzheimer's disease patients with auto mutual information

Carlos Gómez[*1]**, Roberto Hornero**[1]**, Daniel Abásolo**[1]**,**

Alberto Fernández[2] **and Javier Escudero**[1]

[1] Biomedical Engineering Group, E. T. S. Ingenieros de Telecomunicación, University of Valladolid, Camino del Cementerio s/n, 47011-Valladolid, Spain.

[2] Centro de Magnetoencefalografía Dr. Pérez-Modrego, Complutense University of Madrid, Spain.

AUTHOR'S ADDRESS: Carlos Gómez

E.T.S. Ingenieros de Telecomunicación

University of Valladolid

Camino del Cementerio s/n

47011 - Valladolid (Spain)

Tel: +34 983 423000x5589

Fax: +34 983423667

E-mail: cargom@tel.uva.es

Abstract

The aim of the present study was to analyse the magnetoencephalogram (MEG) background activity in patients with Alzheimer's disease (AD), one of the most frequent disorders among elderly population. For this pilot study, we recorded the MEGs with a 148-channel whole-head magnetometer in 20 patients with probable AD and 21 age-matched control subjects. Artefact-free epochs of 3392 samples were analysed with auto mutual information (*AMI*). Average *AMI* decline rates were lower for the AD patients' recordings than for control subjects' ones. Statistically significant differences were found using a Student's *t*-test ($p < 0.01$) in 144 channels. Mean *AMI* values were analysed with a receiver operating characteristic curve. Sensitivity, specificity and accuracy values of 75%, 90.5% and 82.9% were obtained. Our results show that *AMI* estimations of the magnetic brain activity are different in both groups, hence indicating an abnormal type of dynamics associated with AD. This study suggests that *AMI* might help medical doctors in the diagnosis of the disease.

1. Introduction

Magnetoencephalography (MEG) is a non-invasive technique that allows recording the magnetic fields generated by the human brain. To detect the extremely weak brain magnetic signals (femtotesla range), a SQUID (Superconducting QUantum Interference Device) sensor immersed in liquid helium at 4.2 K is used. MEG provides an excellent temporal resolution, orders of magnitude better than in other methods for measuring cerebral activity, as magnetic resonance imaging, single-photon-emission computed tomography and positron-emission tomography [1]. A reasonable spatial resolution on the scalp can also be achieved, although it drastically depends on the source configuration [2]. In addition, magnetic fields are not distorted by the resistive properties of the skull [1]. Nevertheless, the recordings are very sensitive to external artefacts. Thus, the measures must be carried out in a magnetically shielded room.

Alzheimer's disease (AD) is one of the most frequent disorders among elderly population [3] and it is considered the main cause of dementia in western countries [4]. This irreversible brain disorder is characterized by neural loss and the appearance of neurofibrillary tangles and senile plaques. Symptoms of AD are memory loss, confusion, disorientation and speech problems. Although a definite diagnosis is only possible by necropsy, a differential diagnosis with other types of dementia should be attempted. It includes exhaustive medical, neurological, psychiatric and neuropsychological examinations. Diagnostic tools and criteria make possible for physicians to pursue a positive clinical diagnosis of AD with an accuracy of round 80 to 88% [5]. Given the fact that non-linearity is present in the brain, even at the cellular level [6], non-linear analysis of the MEG background activity might be another tool to help physicians in the diagnosis of the disease.

Several authors have analysed EEG/MEG activity in AD patients with non-linear methods. Correlation dimension (D_2) and the first Lyapunov exponent (L_1) are the most widely used. The first one is a static measure of system complexity and characterizes the distribution of points in the phase space [7]. On the other hand, L_1 is a dynamic complexity measure that describes the divergence of trajectories starting at nearby initial states [3]. EEG studies showed that D_2 and L_1 values obtained from AD patients' EEGs were significantly lower than those estimated from control subjects' ones at most electrodes [8, 9]. D_2 was also applied to multichannel MEG data of AD patients in different frequency bands [10]. Other research work suggested that the D_2 reduction is correlated with the dementia severity [11]. Nevertheless, both measures D_2 and L_1 have some drawbacks. First, the algorithms require the time series to be stationary and noise free [12], something that cannot be achieved for physiological data. Moreover, a large quantity of data is necessary to obtain meaningful results [13]. Therefore, other non-linear methods are necessary to analyse the electrical and magnetic brain activity in AD patients. For example, Lempel-Ziv complexity has been applied to EEG and MEG data [14, 15]. With almost the same data set of the current study, p-values lower than 0.01 (Student's t-test) were achieved in all MEG channels [14]. Abásolo et al. [15] found significant differences in the EEG electrodes P3, P4, O1 and T5 with this complexity measure. Other authors analysed AD patients' EEGs with synchronization likelihood and detrended fluctuation analysis [16]. They concluded that spontaneous fluctuations of synchronization were diminished in AD patients in the lower alpha and beta bands. Moreover, an increased regularity was found in the EEG of AD patients using approximate and sample entropies [17, 18]. Approximate entropy was significantly lower in the AD patients at electrodes P3 and P4 [17], whereas significant differences

were found at P3, P4, O1 and O2 with sample entropy [18]. These studies show a neuronal dysfunction associated with AD.

In this paper, MEG activity has been analysed by means of mutual information (*MI*), a measure of the linear and non-linear statistical dependencies between two time series [19]. *MI* and other indexes derived from information theory have been computed to study the brain activity in several physiological and pathological states. Chen et al. [20] suggested that the complexities of almost all information transmissions between different brain areas drop significantly just before and after generalized seizures. Na et al. [21] have investigated the EEG information transmission in schizophrenic patients using cross mutual information (*CMI*). In [22], Lempel-Ziv complexity measures were extracted from the *MI* time series of EEGs in order to predict response during isoflurane anaesthesia. These measures have also been used to investigate evoked activity. *CMI* has been applied to professional perfume researchers, perfume salespersons and general workers' EEGs to investigate the changes of cortico-cortical connectivity during odour stimulation [23]. Furthermore, it has been used to analyse the EEG responses to long-term audio-visual stimulation [24]. AD has also been investigated using some indexes derived from information theory. Benedetti et al. [25] have studied the functional connectivity among different brain regions in AD patients computing *MI* of EEGs. Finally, Jeong el al. [19] have used auto mutual information (*AMI*) and *CMI* to classify AD patients and control subjects' EEGs.

The present study was undertaken to examine the MEG background activity in 20 AD patients and 21 age-matched control subjects with *AMI*, the *MI* between a signal $x(t)$ and the time-delayed time series $x(t+\tau)$. The *AMI* decrease rate with increasing time delays is a measure of the time series regularity [19]. Accepting the notion that the cognitive dysfunction in AD is related to an irregularity loss in the patients' brains [17-

19], our purpose was to test the hypothesis that the MEG regularity is higher in AD patients than in the control group, hence indicating an abnormal type of dynamics associated with this dementia.

2. Methods

MI quantifies the amount of information gained about one signal from the measurement of another. Furthermore, *MI* between two time series is zero when those series are completely independent, while *MI* has a maximum value if both series are equal. This measure is based upon concepts from information theory [26]. Let *X* be a signal with a probability distribution $P_X(x)$. The classical entropy *H* of this signal is the average amount of information gained from any observation of *X*. *H(X)* is known as Shannon's entropy and can be calculated as:

$$H(X) = -\sum_{x_i} P_X(x_i) \cdot \log P_X(x_i)$$

(1)

Given a general coupled system *(X,Y)*, the uncertainty in a measurement of *X* under the condition that *Y* has been measured and found to be y_j is:

$$H(X|Y=y_j) = -\sum_{x_i} P_{XY}(x_i|y_j) \cdot \log P_{XY}(x_i|y_j) =$$
$$= -\sum_{x_i} \frac{P_{XY}(x_i, y_j)}{P_Y(y_j)} \cdot \log \frac{P_{XY}(x_i, y_j)}{P_Y(y_j)}$$

(2)

where $P_{XY}(x_i,y_j)$ is the joint probability density for the measures $X = x_i$ and $Y = y_j$. The uncertainty of *X*, under the condition that *Y* is known, is obtained by averaging the equation (2) over y_j:

$$H(X|Y) = \sum_{y_j} P_Y(y_j) \cdot H(X|Y = y_j)$$

$$= - \sum_{x_i, y_j} P_{XY}(x_i, y_j) \cdot \log \frac{P_{XY}(x_i, y_j)}{P_Y(y_j)} \qquad (3)$$

$$= H(X,Y) - H(Y)$$

where

$$H(X,Y) = - \sum_{x_i, y_j} P_{XY}(x_i, y_j) \cdot \log P_{XY}(x_i, y_j) \qquad (4)$$

MI can be defined as the reduction of the uncertainty of *X* when *Y* is known [27]:

$$I_{XY} = H(X) - H(X|Y) = H(X) + H(Y) - H(X,Y) \qquad (5)$$

Using the definition of Shannon's entropy, the previous equation can be rewritten as follows:

$$I_{XY} = \sum_{x_i, y_j} P_{XY}(x_i, y_j) \cdot \log \frac{P_{XY}(x_i, y_j)}{P_X(x_{ij}) \cdot P_Y(y_j)} \qquad (6)$$

This expression is the cross mutual information (*CMI*) and quantifies the information transmitted from one signal to another [19]. Applied to MEG signals, the *CMI* measures the amount of information transmitted between certain areas of the brain. In our study, we have computed the auto mutual information (*AMI*), the *MI* between one signal $x(t)$ and its time-delayed version $x(t + \tau)$:

$$I_{XX_\tau} = \sum_{x(t), x(t+\tau)} P_{XX_\tau}[x(t), x(t+\tau)] \cdot \log \frac{P_{XX_\tau}[x(t), x(t+\tau)]}{P_X[x(t)] \cdot P_{X_\tau}[x(t+\tau)]} \qquad (7)$$

In order to calculate *AMI* from experimental data, it is necessary to estimate the joint probability density and the probability distributions of *X* and X_τ. In this study, we

have estimated these probabilities from histograms. For a given epoch length, the use of larger sampling bins to construct the histograms produces more accurate estimates of the average probability, but the estimate of the joint probability distribution is too flat, underestimating the *AMI*. On the other hand, the use of smaller bins is better to indicate changes in the joint probability over short distances, but it produces fluctuations due to the small sample size, overestimating the *AMI* [19]. We have used 64 bins to construct the histograms as this value provides stable estimations [19, 21, 23]. The procedure to estimate the probability densities is as follows:

- Histograms of the signal $x(t)$ (Fig. 1a) and its time-delayed version $x(t+\tau)$ were constructed.

- Probability distributions of X and X_τ were obtained as the ratio between the number of samples in each of the 64 bins and the total number of samples [27], as Fig. 1b shows.

- To calculate the joint probability distribution, the (X, X_τ) plane was partitioned into a 64x64 matrix. The joint probability density was obtained dividing the number of samples in each cell of the aforementioned plane by the total number of samples (Fig. 1c).

INSERT FIGURE 1 AROUND HERE

In our research, *AMI* was estimated in all channels over a time delay from 0 to 0.5 seconds. In order to normalize the *AMI* profiles, they were divided by the *AMI* value at $\tau = 0$. Hence, values are in the range between 0 and 1 and *AMI* value at a zero time delay is always one. Finally, the slope of this normalized profile was estimated by a line that fits the data in a least-squares sense. This slope was calculated from $\tau = 0$ to the first

relative minimum value of the profile. Due to the fact that the decline rate of the *AMI* is positively correlated with the entropy [29], this metric might be used to measure the signal regularity.

3. MEG recording

The signals were acquired with a 148-channel whole-head magnetometer (MAGNES 2500 WH, 4D Neuroimaging, San Diego, USA) placed in a magnetically shielded room, during a 5-minute resting period. The subjects lay on a patient bed, in a relaxed state and with their eyes closed. They were asked to stay awake and to avoid making movements. In order to control subjects' performance and to avoid drowsiness effects, their behaviour and level of consciousness was controlled during the whole recording by means of a video-camera. Additionally, technicians may communicate with subjects during measurements using a loud-speaking intercom. Participants included in the final sample did not exhibit significant difficulties in maintaining their immobility.

For each subject, MEGs were recorded with a 678.17 Hz sampling frequency, using a hardware band-pass filter of 0.1-200 Hz. Afterwards, these recordings were decimated, what consisted of filtering the data to respect Nyquist criterion [30], following by a down-sampling by a factor of 4 (169.549 Hz, 50863 samples). Artefact-free epochs of 20 seconds (3392 data points) were selected. Finally, these epochs were filtered between 0.5 and 40 Hz and were copied to a computer as ASCII files for further non-linear analysis.

In the present study, MEG signals were recorded from 41 subjects. Cognitive status was screened in both groups with the Spanish version [31] of Mini Mental State Examination (MMSE) of Folstein et al. [32]. MEGs were obtained from twenty patients (7 men and 13 women; age = 73.05 ± 8.65 years, mean ± standard deviation, SD)

fulfilling the criteria of probable AD. They were recruited from the Asociación de Enfermos de Alzheimer (AFAL). Diagnosis for all patients was made according to the criteria of the National Institute of Neurological and Communicative Disorders and Stroke–Alzheimer's Disease and Related Disorders Association (NINCDS–ADRDA) [33]. The MMSE score for these patients was 17.85 ± 3.91 (mean $\pm$ SD). One of them had a score of less than 12 points, indicating a severe degree of dementia. Patients were free of other significant medical, neurological and psychiatric diseases than AD. Moreover, they were not using drugs which could affect MEG activity when the signals were recorded.

The control group consisted of 21 elderly control subjects without past or present neurological disorders (9 men and 12 women; age $= 70.29 \pm 7.07$ years, MMSE score $= 29.10 \pm 1.00$ points, mean $\pm$ SD). The difference in the mean age of both populations was not statistically significant ($p = 0.26 > 0.01$, Student's t-test). Prior to the MEG recording, all control subjects and all caregivers of the patients signed an informed consent for the participation in this research work. The local Ethics Committee approved this study.

4. Results

In this study, *AMI* profiles were estimated for the 148 MEG channels, with a maximum time delay of 500 milliseconds. For the construction of the histograms, 64 bins were used. Afterwards, these profiles were normalized and their decline rates were calculated from $\tau = 0$ to the first minimum value. Fig. 2a illustrates two of these profiles, one obtained from an AD patient's MEG epoch and other from a control subject's one. This figure shows that *AMI* values decrease quickly for low τ values, then exhibit a transitory oscillation and finally become stable when the time delay values increase.

Enhancements round 0.03 s (control subject) and 0.07 s (AD patient) can be observed in the oscillation part of both profiles. An increase at the inverse of the dominant frequency of each group (6.63 Hz in healthy subjects and 12.17 Hz in AD patients [34]) may be expected if the *AMI* method measures only the lineal statistical dependencies. Nevertheless, as *AMI* provides access to both linear and nonlinear interdependencies, these increases in the profiles are not straightforwardly related to the mean frequency. For each channel, these profiles were averaged, obtaining a normalized *AMI* profile for each group. Fig. 2b represents the normalized profiles for both groups at channel A1. As it can be noticed, absolute values of the *AMI* decrease rate are lower in the AD patients group than in the control subject group. This behaviour is similar for all channels, as Fig. 3 shows. The absolute values of the decline rate were lower in the AD patients group, indicating differences between the non-linear dynamics of AD patients and control subjects' MEGs. Moreover, the differences between AD patients and elderly control subjects were statistically significant in 144 channels ($p < 0.01$, Student's *t*-test). Only in the edge channels A136, A137, A138 and A139, the result of the Student's *t*-test was higher than 0.01.

INSERT FIGURE 2 AROUND HERE

INSERT FIGURE 3 AROUND HERE

After the estimation of the *AMI* decline rate, it was necessary to analyse 148 values for each subject. In this study, the dimensionality of our results has been reduced via principal components analysis (PCA), a well-known technique for dimensionality

reduction [35]. The first principal component provides 83.6% of the total variance explained. Moreover, each of the remaining components explains less than 5%. Therefore, only the first principal component was retained and the first score, projection of the original data onto the first principal component axes, calculated. We analysed the relationship between the first score and the mean *AMI* values, calculated averaging the decline rate from the 148 channels for each subject. With this aim, we computed Pearson's linear correlation coefficient between the first score and the mean *AMI* values. We obtained a 0.999 value, indicating that the strength of association between the variables is very high. Furthermore, as the first principal score provides similar information that the mean *AMI* value, the last one was analysed. Moreover, the evaluation of these mean values allows us an easier interpretation of the results.

The mean *AMI* values were analysed with a ROC curve [36], which summarizes the performance of a two-class classifier across the range of possible thresholds. It is a graphical representation of the trade-offs between sensitivity and specificity. Sensitivity is the true positive rate while specificity is equal to the true negative rate:

$$Sensitivity = \frac{TP}{TP + FN} \tag{8}$$

$$Specificity = \frac{TN}{TN + FP} \tag{9}$$

where false negatives (*FN*) are the AD patients classified as control subjects, and false positives (*FP*) are the controls classified as patients. True positives (*TP*) and true negatives (*TN*) are the patients and control subjects correctly recognized, respectively. Accuracy is a related parameter that quantifies the total number of subjects (AD patients and control subjects) precisely classified:

$$Accuracy = \frac{TP + TN}{TP + TN + FP + FN} \tag{10}$$

Moreover, ROC curves can be used to select the optimal threshold, the best trade-off between specificity and sensitivity. The optimal threshold in our diagnostic test was -0.116, the decrease rate value in which the highest accuracy was obtained. At that point, we obtained accuracy, specificity and sensitivity values of 82.9%, 90.5% and 75% respectively, as it can be noticed in Fig. 4. The area under the ROC curve (AROC) is a single number summary of performance. For a perfect test the area is 1 while an AROC of 0.5 represents a worthless test. We achieved an AROC of 0.883.

INSERT FIGURE 4 AROUND HERE

----

5. Discussion and conclusions

In this study, we have used the *AMI* to study the MEG background activity in 20 patients with probable AD and 21 age-matched control subjects. We have used a value of τ_{max} = 500 milliseconds and 64 bins to construct the histograms. Our purpose was to check the hypothesis that the brain activity recorded in MEG signals is different in AD patients than in control subjects.

The absolute values of the *AMI* decline rate were significantly lower for AD patients in most channels (Student's *t*-test, $p < 0.01$), indicating an abnormal type of dynamics associated with the disease. Given the fact that the decline rate of the *AMI* is positively correlated with the entropy [29] and that entropy measures quantify the regularity of a signal [37, 38], our study suggests that brains affected by AD show a more regular physiological behaviour. Our results are in agreement with previous research works that have applied non-linear methods to study the brain activity in AD patients. These studies revealed less complexity and irregularity in brain recordings of

AD patients than in controls. Most of them were carried out estimating D_2 and L_1, reporting a loss of complexity on brain background activity in AD patients' recordings. Jeong et al. [8] estimated D_2 and L_1 using a method proposed by Kennel et al. [39]. Their results showed significant differences between AD patients and control subjects in almost all EEG channels. Using a larger database, Besthorn et al. [11] suggested that a lower D_2 value was correlated with increased severity of dementia. This measure was also calculated from EEG data and from phase-randomized surrogate data [9]. D_2 values derived from original and surrogate data sets differed significantly in both groups, indicating that this non-linear measure is not simply reflecting spectral properties of the data. Finally, van Cappellen van Walsum et al. [10] estimated the D_2 in different MEG frequency bands. Statistical differences between AD patients and age-matched controls were found in delta, theta and beta bands. A broad band 0.5-40 Hz was also analysed, although this measure revealed no significant differences between both groups. However, for a suitable estimation of D_2 and L_1, stationary and noise-free signals and a large number of data points are needed [12, 13]. These assumptions cannot be fulfilled for physiological data, as EEG and MEG. On the other hand, *AMI* does not require a large number of data points to be reliably estimated and can be applied to non-stationary time series [19]. Thus, this measure is much better suited for MEG analysis than traditional non-linear techniques as L_1 or D_2.

Nowadays, other non-linear methods, which also avoid the drawbacks of classical non-linear measures, have been used to study the EEG/MEG activity. In order to study the regularity of the EEG, approximate and sample entropies have been used. Approximate entropy values were significantly lower in the EEG of AD patients at P3 and P4 electrodes [17]. With sample entropy, significant differences were found at parietal and occipital regions [18]. Jeong et al. [19] found that *AMI* profiles decrease

with time delay slower in the EEGs acquired from severe AD patients than in control subjects' EEGs. These studies showed an increase of the EEG regularity in AD patients compared with control subjects. Our work is in agreement with these EEG studies, but this is the first time that *AMI* and a ROC curve have been used to differentiate the MEGs from AD patients and control subjects.

In addition to D_2 and L_1, other complexity non-linear methods have been used to classify AD patients versus control subjects. The EEG complexity in the Kolmogorov's sense was computed with Lempel-Ziv complexity. Abásolo et al. [15] found that AD patients had significantly lower Lempel-Ziv complexity values at electrodes P3 and O2 with a two-symbol sequence conversion, and at P3, P4, O1 and T5 using three symbols. Their results suggested that a three-symbol conversion might give more detailed insight of the differences between the AD patients and control subjects' EEGs. This complexity measure was also applied to MEG data, obtaining statistically significant differences in all channels [14]. Using multiscale entropy, Escudero et al. [40] concluded that the EEG background activity is less complex in AD patients than control subjects. The results of these studies suggest that the increase in the regularity of the AD patients' brain recordings is associated with a complexity reduction of the brain activity.

Stam et al. [16] examined the fluctuation of the EEG synchronization level of AD patients with detrended fluctuation analysis. They concluded that AD is characterized by diminished fluctuations in the level of synchronization. In other paper, the interdependencies between MEG signals in six frequency bands were studied with synchronization likelihood and coherence [41]. They found changes of long and short distances interaction in the theta, alpha1, beta and gamma bands. These changes may reflect loss of anatomical connections and/or reduced central cholinergic activity and could underlie part of the cognitive impairment [41]. Thus, AD may be characterized

not only by changes in the complexity/irregularity of the brain activity, but also by a lower mean level of functional connectivity as well as by changes in the spontaneous fluctuations of synchronization [16].

Table 1 shows a summary of the papers concerning the classification of AD patients versus control subjects. Nevertheless, the results of these studies cannot be compared because the data sets and the brain recordings (EEG or MEG) are different.

INSERT TABLE 1 AROUND HERE

In addition to these non-linear studies, AD patients' brain activity has been also analysed with spectral measures. Spectral analysis seems to discriminate AD patients from control subjects through an increased EEG/MEG activity in lower frequency bands associated with AD. Signorino et al. [42] found a raise in the EEG powers of delta and theta bands in AD patients compared with control subjects. Other study showed increased slower and reduced faster activity in AD patients' MEGs [43]. Poza et al. [34] analysed MEG recordings from AD patients and healthy controls with five parameters estimated from the power spectral density, finding statistically significant differences with all of them. These results may suggest that the regularity increase in the AD patients' MEGs, found using *AMI*, could be related to a slowing of the brain activity in AD.

A ROC curve was used to assess the ability of the mean *AMI* values to classify AD patients and control subjects. An AROC of 0.883 was obtained. This value indicates the probability that a randomly selected AD patient of our study has a mean *AMI* value higher than a control subject chosen randomly. The ROC curve was also used to select the optimal threshold (-0.116), the *AMI* decrease rate that provides the highest accuracy.

At this value, specificity of 90.5% (ratio of control subjects properly classified), and sensitivity of 75% (percentage of AD patients correctly identified), were obtained. Our results show that *AMI* method and ROC curves could be used to help physicians in AD diagnosis. Nevertheless, this is a pilot study and further analyses are necessary to confirm our results.

In previous studies, non-linear methods and ROC curves have been used to distinguish AD patients and control subjects. With almost the same data set (21 AD patients and 21 control subjects), the first principal score from Lempel-Ziv complexity results was analysed with a ROC curve [14]. Accuracy values achieved in both studies are very similar (82.9% with *AMI* and 83.3% with Lempel-Ziv complexity). In EEG studies the accuracies obtained are lower in most papers: 81.8% using Lempel-Ziv complexity [15], 77.3% with sample entropy [18] and 69.5% using D_2 [44]. On the other hand, the highest accuracy value (90.1%) was obtained at EEG electrode Fp1 with multiscale entropy [40]. Nevertheless, these values should be taken with caution due to the small sample sizes.

The regularity increase in the MEG of AD patients could be explained by a decreased of dynamic complexity of part of the brain. Nevertheless, the implications of this decreased irregularity in AD patients are not clear. It might be due to neuronal death, a loss of dynamical brain responsivity to stimuli, a general effect of neurotransmitter deficiency or a loss of connectivity of local neural networks as a result of nerve cell death [3, 9]. Because both groups were carefully matched for age, the significantly reduced *AMI* decline rate may represent the cognitive dysfunction in AD.

Our study shows that *AMI* may be an adequate and fast method to differentiate the MEG activity from AD patients and control subjects. Nevertheless, some limitations of our study merit consideration. Firstly, the sample size is small to obtain decisive results.

Thus, a larger database is needed to confirm the performance of our method. Secondly, our results do not show if *AMI* can detect a gradation of the disease process. Therefore, future studies are necessary to analyse MEGs from patients with different stages of AD and with Mild Cognitive Impairment. Finally, changes in EEG/MEG activity also appear in other pathological states as schizophrenia [21], vascular dementia [45] and epilepsy [46].

In summary, this paper presents the *AMI* as a method to study the MEG background activity. We have obtained significant differences between AD patients' recordings and elderly control subjects' MEGs. Our findings show the usefulness of this measure to detect changes in the dynamical behaviour of brains injured by the development of AD.

References

[1] M. Hämäläinen, R. Hari, R.J. Ilmoniemi, J. Knuutila and O.V. Lounasmaa, Magnetoencephalograpy – theory, instrumentation, and applications to noninvasive studies of the working human brain, Rev. Mod. Phys. 65 (1993) 413–497.

[2] R. Hari and N. Forss, Magnetoencephalography in the study of human somatosensory cortical processing, Phil. Trans. R. Soc. Lond. B 354 (1999) 1145–1154.

[3] J. Jeong, EEG dynamics in patients with Alzheimer's disease, Clin. Neurophysiol. 115 (2004) 1490–1505.

[4] T.D. Bird, Alzheimer's disease and other primary dementias, in Harrison's principles of internal medicine, eds. E. Braunwald, A.S. Fauci, D.L. Kasper, S.L. Hauser, D.L. Longo and J.L. Jameson, pp. 2391–2399 (The McGraw-Hill Companies Inc., New York NY, 2001).

[5] E.J. Jonkman, The role of the electroencephalogram in the diagnosis of dementia of the Alzheimer type: an attempt at technology assessment, Neurophysiol. Clin. 27 (1997) 211–219.

[6] R.G. Andrzejak, K. Lehnertz, F. Mormann, C. Rieke, P. David and C.E. Elger, Indications of nonlinear deterministic and finite-dimensional structures in time series of brain electrical activity: Dependence on recording region and brain state, Phys. Rev. E 64 (2001) 061907.

[7] R. Hornero, A. Alonso, N. Jimeno, A. Jimeno and M. López, Nonlinear analysis of time series generated by schizophrenic patients, IEEE Eng. Med. Biol. 18 (1999) 84–90.

[8] J. Jeong, S.J. Kim and S.H. Han, Non-linear dynamical analysis of the EEG in Alzheimer's disease with optimal embedding dimension, Electroenceph. clin. Neurophysiol. 106 (1998) 220–228.

[9] B. Jelles, J.H. van Birgelen, J.P.J. Slaets, R.E.M. Hekster, E.J. Jonkman and C.K. Stam, Decrease of non-linear structure in the EEG of Alzheimer patients compared to healthy controls, Clin. Neurophysiol. 110 (1999) 1159–1167.

[10] A.M. van Cappellen van Walsum, Y.A.L. Pijnenburg, H.W. Berendse, B.W. van Dijk, D L. Know, Ph. Scheltens and C.J. Stam, A neural complexity measure applied to MEG data in Alzheimer's disease, Clin. Neurophysiol. 114 (2003) 1034–1040.

[11] C. Besthorn, H. Sattel, C. Geiger-Kabisch, R. Zerfass and H. Förstl, Parameters of EEG dimensional complexity in Alzheimer's disease, Electroenceph. clin. Neurophysiol. 95 (1995) 84–89.

[12] P. Grassberger and I. Procaccia, Characterization of strange attractors, Phys. Rev. Lett. 50 (1983) 346–349.

[13] J.P. Eckmann and D. Ruelle, Fundamental limitations for estimating dimensions and Lyapunov exponents in dynamical systems, Physica D 56 (1992) 185–187.

[14] C. Gómez, R. Hornero, D. Abásolo, A. Fernández and M. López, Complexity analysis of the magnetoencephalogram background activity in Alzheimer's disease patients, Med. Eng. Phys. 28 (2006) 851–859.

[15] D. Abásolo, R. Hornero, C. Gómez, M. García and M. López, Analysis of EEG background activity in Alzheimer's disease patients with Lempel–Ziv complexity and central tendency measure, Med. Eng. Phys. 28 (2006) 315–322.

[16] C.J. Stam, T. Montez, B.F. Jones, S.A.R.B. Rombouts, Y. van der Made, Y.A.L. Pijnenburg and Ph. Scheltens, Disturbed fluctuations of resting state EEG synchronization in Alzheimer's disease, Clin. Neurophysiol. 116 (2005) 708–715.

[17] D. Abásolo, R. Hornero, P. Espino, J. Poza, C.I. Sánchez and R. de la Rosa, Analysis of regularity in the EEG background activity of Alzheimer's disease patients with Aproximate Entropy, Clin. Neurophysiol. 116 (2005) 1826–1834.

[18] D. Abásolo, R. Hornero, P. Espino, D. Álvarez and J. Poza, Entropy analysis of the EEG background activity in Alzheimer's disease patients, Physiol. Meas. 27 (2006) 241–253.

[19] J. Jeong, J.C. Gore and B.S. Peterson, Mutual information analysis of the EEG in patients with Alzheimer's disease, Clin. Neurophysiol. 112 (2001) 827–835.

[20] F. Chen, J. Xu, F. Gu, X. Yu, X. Meng and Z. Qiu, Dynamic process of information transmission complexity in human brains, Biol. Cybern. 83 (2000) 355–366.

[21] S.H. Na, S.H. Jin, S.Y. Kim and B.J. Ham, EEG in schizophrenic patients: mutual information analysis, Clin. Neurophysiol. 113 (2002) 1954–1960.

[22] L. Huang, P. Yu, F. Ju and J. Cheng, Prediction of response to incision using mutual information of electroencephalograms during anaesthesia, Med. Eng. Phys. 25 (2003) 321–327.

[23] B.C. Min, S.H. Jin, I.H. Kang, D.H. Lee, J.K. Kang, S.T. Lee and K. Sakamoto, Analysis of mutual information content for EEG responses to odor stimulation for subjects classified by occupation, Chem. Senses 28 (2003) 741–749.

[24] M. Teplan, A. Krakovská and S. Stolc, EEG responses to long-term audio–visual stimulation, Int. J. Psychophysiol. 59 (2006) 81–90.

[25] F. Benedetti, C. Arduino, S. Costa, S. Vighetti, L. Tarenzi, I. Rainero and G. Asteggiano, Loss of expectation-related mechanisms in Alzheimer's disease makes analgesic therapies less effective, Pain 121 (2006) 133–144.

[26] C.E. Shannon and W. Weaver, The Mathematical Theory of Communication (University of Illinois Press, Urbana IL, 1949).

[27] F. Rossi, A. Lendasse, D. François, V. Wertz and M. Verleysen, Mutual information for the selection of relevant variables in spectrometric nonlinear modelling, Chemometr. Intell. Lab. Syst. 80 (2006) 215–226.

[28] E. Pereda, R.Q. Quiroga and J. Bhattacharya, Nonlinear multivariate analysis of neurophysiological signals, Prog. Neurobiol. 77 (2005) 1–37.

[29] M. Palus, Coarse-grained entropy rates for characterization of complex time series, Physica D 93 (1993) 64–77.

[30] A.V. Oppenheim and R.W. Schafer Digital Signal Processing (Prentice Hall Inc., New Jersey NJ, 1975).

[31] A. Lobo and V. Ezquerra, El mini-examen cognoscitivo: un test sencillo y práctico para detectar alteraciones intelectivas en pacientes médicos, Actas Luso-Españolas de Psiquiatría y Psicología Médica 3 (1973) 189–202.

[32] M.F. Folstein, S.E. Folstein and P.R. McHugh, Mini-mental state: A practical method for grading the cognitive state of patients for the clinician, J. Psychiatr. Res. 12 (1975) 189–198.

[33] G. McKhann, D. Drachman and M. Folstein, Clinical diagnosis of Alzheimer's disease: report of NINCDS–ADRDA work group under the auspices of department of health and human services task force on Alzheimer's disease, Neurology 34 (1984) 939–944.

[34] J. Poza, R. Hornero, D. Abásolo, A. Fernández and M. García, Extraction of spectral based measures from MEG background oscillations in Alzheimer's disease, Med. Eng. Phys. (2006), Article in press, doi: 10.1016/j.medengphy.2006.11.006.

[35] I.T. Jolliffe, Principal Component Analysis (Springer-Verlag, New York NY, 1986).

[36] M.H. Zweig and G. Campbell, Receiver-operating characteristic (ROC) plots: a fundamental evaluation tool in clinical medicine, Clin. Chem. 39 (1993) 561–577.

[37] M. Costa, A.L. Goldberger and C.K. Peng, Multiscale entropy analysis of complex physiologic time series, Phys. Rev. Lett. 89 (2002) 068102.

[38] S.M. Pincus, I.M. Gladstone and R.A. Ehrenkranz, A regularity statistic for medical data analysis, J. Clin. Monit. 7 (1991) 335–345.

[39] M.B. Kennel, R. Brown and H.D.I. Abarbanel, Determining embedding dimension for phase-space reconstruction using a geometrical construction, Phys. Rev. A 45 (1992) 3403–3411.

[40] J. Escudero, D. Abásolo, R. Hornero, P. Espino and M. López, Analysis of electroencephalograms in Alzheimer's disease patients with multiscale entropy, Physiol. Meas. 27 (2006) 1091–1106.

[41] C.J. Stam, B.F. Jones, I. Manshanden, A.M. van Cappellen van Walsum, T. Montez, J.P.A. Verbunt, J.C. de Munck, B.W. van Dijk, H.W. Berendse and Ph. Scheltens, Magnetoencephalographic evaluation of resting-state functional connectivity in Alzheimer's disease, Neuroimage 32 (2006) 1335–1344.

[42] M. Signorino, E. Pucci, N. Belardinelli, G. Nolle and F. Angeleri, EEG spectral analysis in vascular and Alzheimer dementia, Electroenceph. clin. Neurophysiol. 94 (1995) 313–325.

[43] D. Osipova, J. Ahveninen, O. Jensen, A. Ylikoski and E. Pekkonen, Altered generation of spontaneous oscillations in Alzheimer's disease, Neuroimage 27 (2005) 835–841.

[44] C. Besthorn, R. Zerfass, C. Geiger-Kabisch, H. Sattel, S. Daniel, U. Schreiter-Gasser and H. Förstl, Discrimination of Alzheimer's disease and normal aging by EEG data, Electroenceph. clin. Neurophysiol. 103 (1997) 241–248.

[45] J. Jeong, J.H. Chae, S.Y. Kim and S.H. Han, Nonlinear dynamic analysis of the EEG in patients with Alzheimer's disease and vascular dementia, J. Clin. Neurophysiol. 18 (2001) 58–67.

[46] H. Jing and M. Takigawa, Comparison of human ictal, interictal and normal non-linear component analyses, Clin. Neurophysiol. 111 (2001) 1282–1292.

TABLES

Table 1. Summary of the papers, in alphabetical order, concerning the classification of AD patients versus control subjects with non-linear methods: approximate entropy (*ApEn*), Lempel-Ziv complexity (*LZC*), sample entropy (*SampEn*), correlation dimension (D_2), multiscale entropy (*MSE*), first Lyapunov exponent (L_1), auto mutual information (*AMI*), cross-mutual information (*CMI*), synchronization likelihood (*SL*) and detrended fluctuation analysis (*DFA*).

Paper	Data set	Method	Results
Abásolo et al. 2005 [17]	10 AD patients and 8 control subjects (EEG)	*ApEn*	AD patients' EEGs showed significantly lower *ApEn* values than control subjects at P3 and P4 ($p<0.01$). They obtained 70% sensitivity and 100% specificity at P3, and 80% sensitivity and 75% specificity at P4.
Abásolo et al. 2006 [15]	11 patients with AD and 11 control subjects (EEG)	*LZC*	Significant differences were found at P3 and O2 with a two-symbol sequence conversion (accuracy values of 81.8% at both electrodes), and at P3, P4, O1 and T5 using three symbols (accuracy of 81.8% at P3, P4 and O1, and of 72.7% at T5).
Abásolo et al. 2006 [18]	11 AD patients and 11 control subjects (EEG)	*SampEn*	*SampEn* was significantly lower in the AD patients at electrodes P3, P4, O1 and O2 ($p<0.01$). Accuracy values of 77.3% were obtained at those electrodes.
Besthorn et al. 1995 [11]	50 AD patients and 42 controls (EEG)	D_2	This study showed that a lower D_2 was correlated with increased severity of dementia.
Besthorn et al. 1997 [44]	50 AD patients and 42 control subjects (EEG)	D_2	Using D_2, AD patients and control subjects were correctly classified with an accuracy of 69.5%.
Escudero et al. 2006 [40]	11 AD patients and 11 control subjects (EEG)	*MSE*	Using *MSE*, AD patients had significantly lower complexity than control subjects at F3, F7, Fp1, Fp2, T5, T6, P3, P4, O1 and O2 ($p<0.01$). The highest accuracy value was obtained at electrode Fp1: 90.9%.
Gómez et al. 2006 [14]	21 patients with AD and 21 elderly control subjects (MEG)	*LZC*	MEG signals from AD patients had significantly lower *LZ* complexity than control subjects' MEGs at all channels ($p<0.01$). Specificity of 85.7%, sensitivity of 80.9% and accuracy of 83.3% were obtained when the first principal score from PCA was analysed with a ROC curve.
Jelles et al. 1999 [9]	24 AD patients and 22 controls (EEG)	D_2	D_2 was significantly lower in the AD patients compared to control subjects.
Jeong et al. 1998 [8]	12 AD patients and 12 control subjects (EEG)	D_2 and L_1	L_1 average values of the EEGs were higher for the normal controls than for the AD patients at all electrodes with the exception of the occipital ones.

			Using D_2, statistically differences were found at all channels excluding F7 and O1.
Jeong et al. 2001 [19]	15 patients with AD and 15 control subjects (EEG)	*AMI* and *CMI*	The *AMI* profiles decreased more slowly in AD patients than in controls. Differences were statistically significant in all channels with the exception of O2. Moreover, the local *CMI* in AD patients was lower than control subjects.
Stam et al. 2005 [16]	24 AD patients and 19 control subjects (EEG)	*SL* and *DFA*	AD is characterized both by a lower mean level of functional connectivity as well as by diminished fluctuations in the level of synchronization.
Stam et al. 2006 [41]	18 AD patients and 18 control subjects (MEG)	*SL*	In the α-1 and β bands, AD patients showed a loss of long distance intrahemispheric interactions, with a focus on left fronto-temporal/ parietal connections. Functional connectivity was increased in AD patients locally in the θ band (centro-parietal regions) and in the β and γ bands (occipito-parietal regions).
Van Cappellen van Walsum et al. 2003 [10]	20 AD patients and 20 control subjects (MEG)	D_2	Mean D_2 was lower in AD patients compared with control subjects at 2–4 and 4–8 Hz frequency bands ($p<0.01$), whereas in the 14–20 and 20–30 Hz bands the mean D_2 was higher in AD patients ($p<0.01$).
Current study	20 patients with AD and 21 elderly control subjects (MEG)	*AMI*	The absolute values of the *AMI* decline rate were significantly lower for AD patients in most channels. An accuracy value of 82.9% was obtained when the mean *AMI* values were analysed with a ROC curve.

Fig. 1. (a) Example of MEG epoch: time series $x(t)$; (b) Probability distributions of X and X_τ from histograms; (c) Histogram of the joint probability distribution.
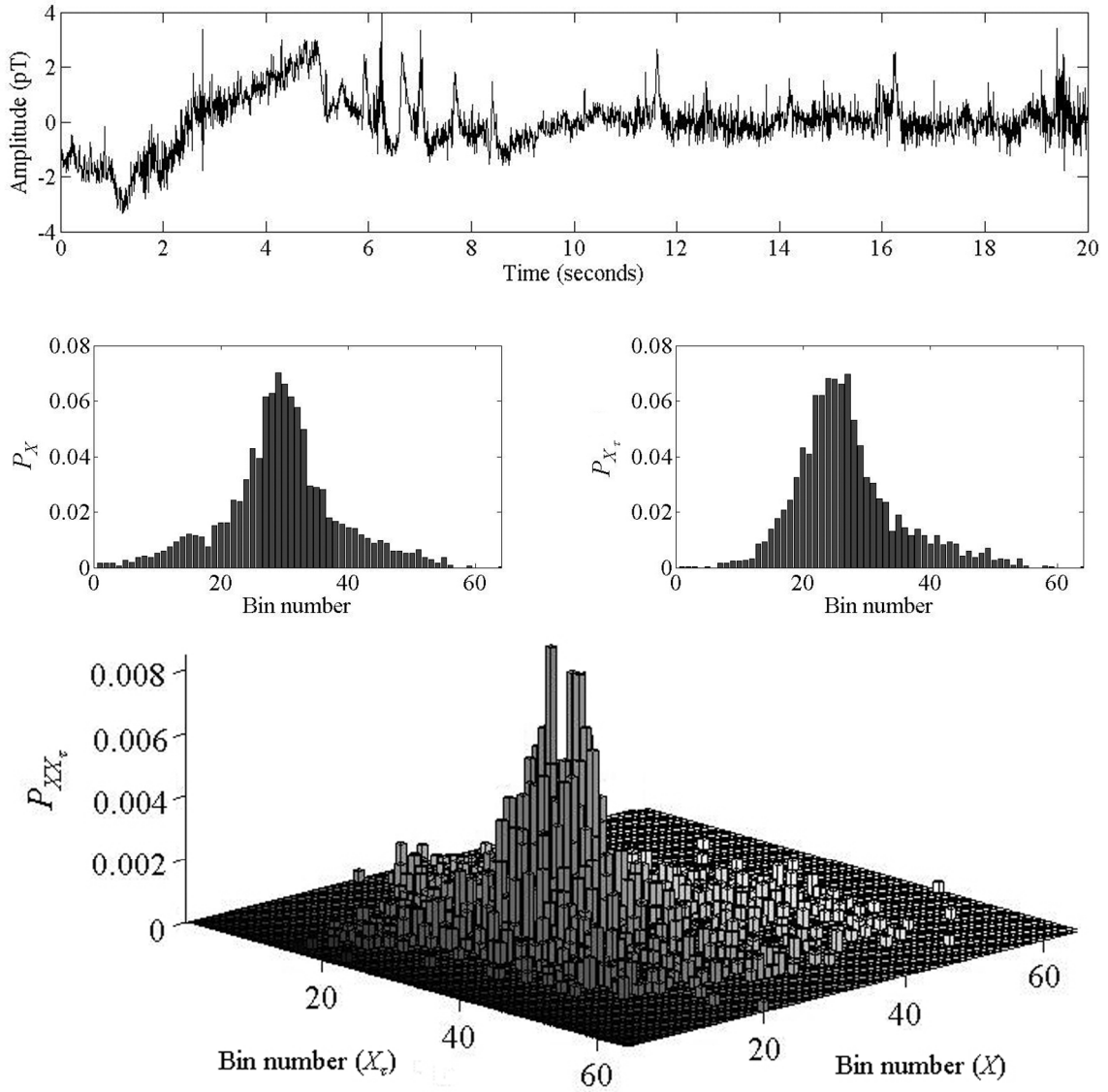
Fig. 2. Normalized *AMI* profiles for (a) one AD patient's epoch and a control subject's epoch and (b) for the 20 AD patients and the 21 control subjects at channel A1 (Central region).
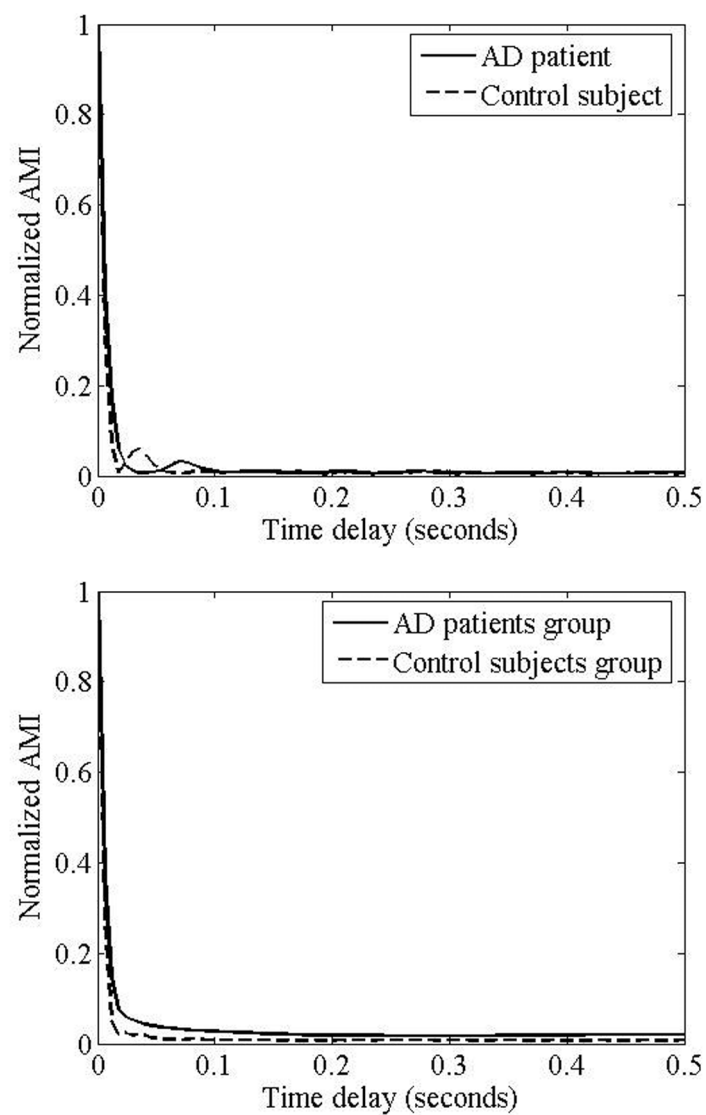
Fig. 3. Averaged *AMI* decrease rate values for the patients with AD and the control subjects in all channels (from A1 to A148).
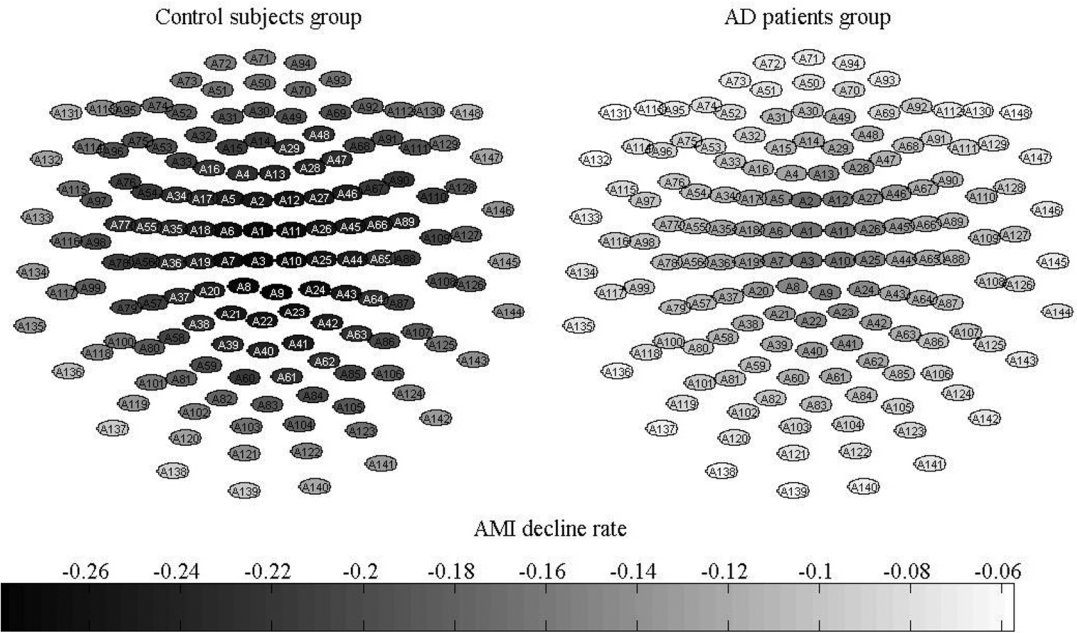
Fig. 4. ROC curve for the mean *AMI* values, obtained from the *AMI* decrease rates at all channels. The optimum cut-off point is marked with a solid circle.